Softening of Cosserat sensitivity in a foam: warp effects

Roderic S. Lakes

Department of Engineering Physics, Engineering Mechanics Program
Department of Materials Science, Rheology Research Center,
University of Wisconsin, 1500 Engineering Drive, Madison, WI 53706-1687

Abstract

Buckling gives rise to softening of the structural stiffness of columns; buckling of ribs gives rise to softening of the incremental elastic modulus of foams. Softening of Cosserat characteristic lengths occurs in pre-compressed foam material as determined from warp of cross sections of a square bar in torsion. Warp in the foam is reduced considerably in comparison with the predictions of classical elasticity. Pre-compression increases the warp in comparison with the warp observed without pre-compression. The effect is attributed to release of energy stored via pre-compression.

1 Introduction

1.1 Stability of classical solids

Elastic instability is a well established subject [1]. Buckling of columns is well known. It is also known that the ribs in foam materials can undergo buckling, giving rise to a nonlinear curve of stress vs. strain [2] in which the effective modulus softens above 5% to 10% compressive strain.

Elastic instability can give rise to negative effective properties. In stable elastic systems, an applied deformation gives rise to a restoring force that resists the imposed motion. The ratio of force to displacement represents a spring constant or structural stiffness. The associated ratio of stress to strain within the material represents an elastic modulus. Negative stiffness or negative modulus is associated with instability. A classic example is a flexible column buckled to a sigmoid shape and constrained at the inflection point [1]. If one moves the constraint point while controlling its displacement, a curve of negative structural stiffness can be obtained.

Stability conditions for classical elastic materials [3] are traditionally obtained using the concept of positive definite strain energy density. For classical elasticity, the shear modulus is positive, $G > 0$ and the bulk modulus B is positive, $3B = 3\lambda + 2G > 0$ with λ as a Lamé constant. For an unconstrained block of a classical solid to be stable, the elastic moduli must be positive. The corresponding range for Poisson's ratio ν is $-1 < \nu < \frac{1}{2}$. An assumption of strong ellipticity is required for stability of objects constrained at their surfaces. For classical isotropic elasticity the conditions are $G > 0$; $\lambda + 2G > 0$, allowing the bulk modulus to be negative. Strong ellipticity is associated with the requirement that waves have a real velocity. Strong ellipticity involves a weaker constraint on the elastic constants than positive definite strain energy. An isotropic elastic solid with a negative shear modulus or a negative bulk modulus will have a negative structural rigidity

so such an object with stress-free surfaces is unstable. If the object is constrained at its surfaces, the condition for stability is that of strong ellipticity which allows negative bulk modulus.

Negative elastic moduli are predicted via the classic Landau [4] theory of phase transformation. In a regime in which a material is stable, an energy function of strain and temperature initially has a single minimum corresponding to a positive elastic modulus. As temperature is lowered, the energy function gradually flattens, then it develops two minima with a relative maximum between them. The relative maximum corresponds to a negative elastic modulus which entails instability. The instability is manifested by a transformation of the material to a different crystalline form.

Negative properties of constituents in discrete systems and in composites have been used to obtain extremely high values of properties. This was done by partially constraining the unstable portion within a stable portion. As for structural damping, buckled tubes [5] were used as negative stiffness elements to obtain high viscoelastic damping. Stiffer dampers with a superior figure of merit were made using columns that tilted at the ends during buckling [6]. As for composite materials, analysis predicts large damping peaks and sigmoid shaped anomalies in the modulus in composites containing a partially constrained negative stiffness phase [7]. Such effects were observed in composites containing inclusions in the vicinity of a phase transformation [8]; stiffness greater than that of diamond [9] was observed over a range of temperature.

In foam materials, buckling of rib elements in the foam gives rise to an instability beyond 5% to 10% compressive strain. Buckling of ribs, in addition to altering the shape of the stress strain curve, also gives rise to bands of heterogeneous deformation in the foam [10]. The bands, transverse to the applied load, are apparent to the unaided eye. This phenomenon is understood in the context of negative incremental stiffness of the individual cells, observed experimentally [10].

Stability conditions for Cosserat [11] [12] materials are also obtained using the concept of positive definite strain energy density [13]. Cosserat [11] or micropolar [13] solids incorporate freedom of rotation of points as well as translation, and allow couple stress (moment per area) as well as force stress (force per area). Cosserat solids are predicted to exhibit lower stress concentrations than classical elastic materials [14]. For finite size objects of a Cosserat solid, less stringent conditions may apply [15]. Specifically, negative values of rotation sensitivity coefficients can be associated with a positive structural stiffness provided the object is sufficiently large in size.

Reduction in elastic constants or negative elastic constants can arise if there is stored energy in a material. For example in the alpha to beta phase transition in quartz, the bulk modulus softens considerably [16] via energy that is stored in interatomic forces as temperature is changed. In the present study, energy is stored by axial pre-compression of a foam material. Cosserat elastic constants are probed as a function of pre-compression by measurements of the warp of a square cross section bar in torsion.

1.2 Analysis

Foams and rib lattices exhibit nonclassical elastic behavior: size effects in bending and torsion as well as reductions of stress or strain concentrations compared with classical predictions. Such nonclassical effects have been interpreted via Cosserat elasticity for which exact analytical solutions are available for the interpretation of experiments.

The constitutive equations for linear isotropic Cosserat elasticity are:

$$\sigma_{ij} = 2G\epsilon_{ij} + \lambda\epsilon_{kk}\delta_{ij} + \kappa e_{ijk}(r_k - \phi_k) \tag{1}$$

$$m_{ij} = \alpha\phi_{k,k}\delta_{ij} + \beta\phi_{i,j} + \gamma\phi_{j,i}. \tag{2}$$

The points in the Cosserat continuum have rotational freedom ϕ_m, called micro-rotation which may differ from $r_k = \frac{1}{2}e_{klm}u_{m,l}$ which is the "macro" rotation based on the antisymmetric part of

2

gradient of displacement u_i. e_{jkm} is the permutation symbol. The Cauchy stress σ_{ij} (force per unit area) in Cosserat elasticity can be asymmetric, in contrast to classical elasticity. Cosserat theory incorporates a couple stress m_{ij} (a torque per unit area) which balances the distributed moment associated with asymmetric stress.

The six Cosserat elastic constants are λ, G, α, β, γ, κ. Constants λ and G have the same meaning as in classical elasticity. G is the shear modulus in the absence of gradients. Constants α, β, γ allow sensitivity to rotation gradient. The Cosserat constant κ quantifies the coupling between local rotation and the rotation associated with displacement gradients. The characteristic length for torsion is defined as $\ell_t = \sqrt{\frac{\beta+\gamma}{2G}}$. The characteristic length for bending is defined as $\ell_b = \sqrt{\frac{\gamma}{4G}}$. The dimensionless coupling number is defined as $N = \sqrt{\frac{\kappa}{2G+\kappa}}$. Microstructure or micromorphic elasticity has more freedom [18] [19] and incorporates 18 isotropic elastic constants. Solutions for interpreting quasi-static experiments with micromorphic theory are not available.

For Cosserat solids, an assumption of positive definite strain energy [13] gives rise to $\kappa > 0$; $\gamma > 0$; $-\gamma < \beta < \gamma$; $3\alpha + \beta + \gamma > 0$. These imply $\ell_b^2 > 0$, $\ell_t^2 > 0$ and $N^2 > 0$. In the strain energy analysis there is the further assumption that terms containing elastic constants are independent and uncoupled.

In an object of finite nonzero size, the variables are in fact coupled, so stability conditions for Cosserat solids may not be so stringent [15] as reported above. Indeed, the structural stiffness of bars in torsion and bending can be positive even if some parameters are negative provided the bar is not too thin. Negative or reduced Cosserat elastic constants, as in the classical case, are predicted if stored energy is provided. Moreover, the less stringent condition of strong ellipticity has been considered for Cosserat solids [20].

It is possible to determine all six isotropic Cosserat elastic constants via size effect measurements in torsion and bending [21]. A nonzero structure size does not necessarily imply Cosserat effects; a composite of aluminum beads in an epoxy matrix was found via size effect experiments to be classical [21]. Analysis of composites containing stiff spheres revealed characteristic lengths of zero [22], hence classical behavior, consistent with experiments. The six Cosserat constants were determined for a dense isotropic polymer foam [23] and for low density foam [24]. The Cosserat characteristic length was found experimentally for a 2D polymer honeycomb [25]. Analysis of 2D chiral honeycombs disclosed a Cosserat characteristic length comparable to the cell size [26]. Planar bars with an array of circular holes exhibited size effects in bending [27] from which the characteristic length was found to be on the order of the hole spacing. A wave dispersion study of a non-cohesive granular assembly of metal spheres [28] allowed inference of a value of κ but characteristic lengths were not determined. Large size effects of a factor 30 in stiffness were observed in a rib lattice designed for strong effects [29].

1.2.1 Warp in torsion

Torsion of a bar of square cross section gives rise to warp of the cross sections. The warp, for torsion of a classically linear elastic bar [3] about the z axis, is

$$u_z = \theta[xy - \sum_{n=0}^{\infty} B_n sinh(k_n y)sin(k_n x)]. \tag{3}$$

in which $k_n = (2n+1)\pi/A$ and $B_n = 8(-1)^n/Ak_n^3 cosh(k_n A/2)$, A is the bar width, and θ is twist angle per length. This warp is associated with a concentration of strain with maximum strain at the center of the free surfaces. There is no stress or strain at the corners of a cross section. The

corners have two orthogonal surfaces that are free of stress. Symmetry of the stress implies the shear stress is zero at the corners.

The warp of a Cosserat solid is given [30] for $N = 1$ by an approximate polynomial solution

$$\frac{u_z(x,y)}{\theta a^2/16} = \frac{10 \left(38 + 2211\bar{\ell}_t^2 + 2772\bar{\ell}_b^2\right)\left(x^3 y - xy^3\right) + 33\left(2 - 315\bar{\ell}_t^2\right)\left(x^5 y - xy^5\right)}{4\left(19 + 465\bar{\ell}_t^2 + 990\bar{\ell}_t^4\right) + 742.5\left(6 + 49\bar{\ell}_t^2\right)\bar{\ell}_b^2}. \tag{4}$$

in which $\bar{\ell}_t = \ell_t/a$ and $\bar{\ell}_b = \ell_b/a$ with a as the cross-section half-width and θ as the twist angle per unit length. In Equation (4), x and y are also normalized by a, the bar half-width.

This equation applies for linear isotropic Cosserat elasticity. For the relatively small strain levels applied in torsion, the response is considered a linear perturbation upon the nonlinear buckling that occurs in superposed pre-compression.

Foams often exhibit anisotropy, and the pre-compressed foam has anisotropy induced by the pre-compression. Any moduli inferred from a single experiment are meaningful, but they do not fully characterize the material. Cosserat elastic constants in the present effort are interpreted as technical constants applicable only to the direction studied; for other directions, they may be different as a result of anisotropy. The same approach has been taken with other anisotropic materials. A full solution for anisotropic Cosserat elasticity that might be used for a more comprehensive experimental protocol, is not available.

Warp is reduced in a Cosserat solid compared with a classical solid and the concentration of strain is also reduced. The reduction in warp is greater for larger torsion characteristic length ℓ_t and for larger coupling number N. The bending characteristic length ℓ_b also contributes to the reduction in warp and it changes the shape of the warp curve. The corners of a cross section can experience stress and strain. Stress need not be symmetric in a Cosserat solid. The reduction in warp and corner strain effects have been demonstrated experimentally in foams [31] and in bone.
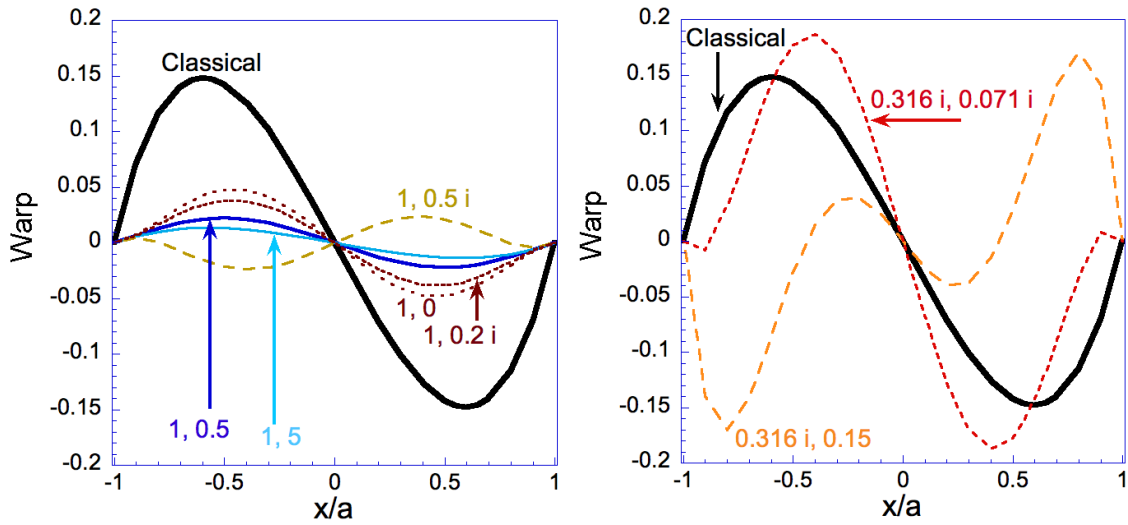

Figure 1: Normalized warp $\frac{u_z(x,y)}{\theta a^2}$ in torsion of a square cross section bar for various Cosserat rotation gradient sensitivity constants including negative values. Number pairs are assumed values of $\bar{\ell}_t$, $\bar{\ell}_b$. The classical elastic warp is shown for comparison.

Now consider materials that contain stored energy that can give rise to instability. The characteristic lengths appear to the second power or higher. So negative $\beta + \gamma$ implies negative ℓ_t^2

assuming a positive modulus. Warp curves assuming various elastic constants including negative values are shown in Figure 1. The warp curves in the left diagram are for normalized torsion characteristic length $\bar{\ell}_t = 1$. Solid curves are for normalized bending characteristic lengths in the range for stability, $\bar{\ell}_b = 0.5$ and 5 respectively. Broken curves are for negative values of γ: $\bar{\ell}_b = 0$, $0.2\,i$ and $0.5\,i$ (with $i = \sqrt{-1}$) corresponding to $\bar{\ell}_b^2 = 0$, -0.04, and -0.25. Relaxing the requirement of positive definite strain energy can reverse the direction of warp but does not always do so. The classical warp is shown for comparison.

The warp curves in the right diagram in Figure 1 are for normalized torsion characteristic length $\bar{\ell} = 0.316\,i$, corresponding to $\bar{\ell}^2 = -0.1$, outside the range allowed for positive definite strain energy. Assuming also $\bar{\ell}_b = 0.15$ results in a wiggly warp curve. Assuming $\bar{\ell}_b = 0.071\,i$ ($\bar{\ell}_b^2 = -0.005$) results in a warp that is similar to the classical curve in shape but is of larger magnitude. Even though these parameters violate the assumption of positive definite strain energy, bars of nonzero size can exhibit positive structural stiffness, hence be stable [15].

2   Methods

Warp of cross sections during torsion of square bars of compliant materials such as rubber of foam is readily apparent to the unaided eye. It is also evident that foams with larger cells warp less than foams with smaller cells or homogeneous materials such as rubber. For the present experiment, a large specimen of foam with large cells was chosen to facilitate measurements and to evoke large effects.
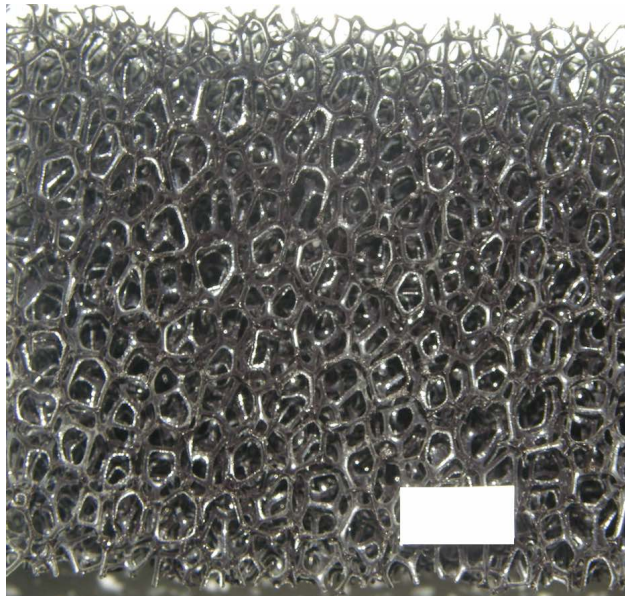

Figure 2: Image of open cell foam. Scale bar length is 10 mm.

Bars of open cell reticulated polyurethane foam from Foamex Industries [17] were used. They were 50 mm in square cross section and about 160 mm long. The foam had a cell size of about 6 mm (Figure 2). The mass and dimensions of each bar were measured. Each end was cemented to a calibrated rotation stage, Newport type 472, supported on an optical breadboard. Fiducial cross section lines were drawn on the foam with ink or acrylic paint. Displacement of the surface was

measured via digital photography. A digital camera was mounted at a right angle to the specimen surface.

Torsion was achieved by applying equal and opposite rotations via the rotation stages. The maximum shear strain was 5% or below, well within the linear range for this class of foam. Digital photographs were taken before and after torsion. Displacements were measured on the images via GIMP image processing software. No averaging or smoothing was done. Pixel count was converted to displacement using the known width of the bar. Tilt deformation of the lateral surfaces was subtracted out.

The experiments were done with no axial pre-compression, and again following axial pre-compression of 0%, 10%, 15%, 20%, 25% and 27% strain. Curve fits to Equation (4) were done for the torsion characteristic length ℓ_t assuming $\ell_b = 0.5\ell_t$. A coupling number $N = 1$ is supported by prior experiments on similar reticulated foam. The bending length ℓ_b has an effect on the shape of the theoretical curves [30] but the data for this foam exhibit too much scatter to infer ℓ_b.
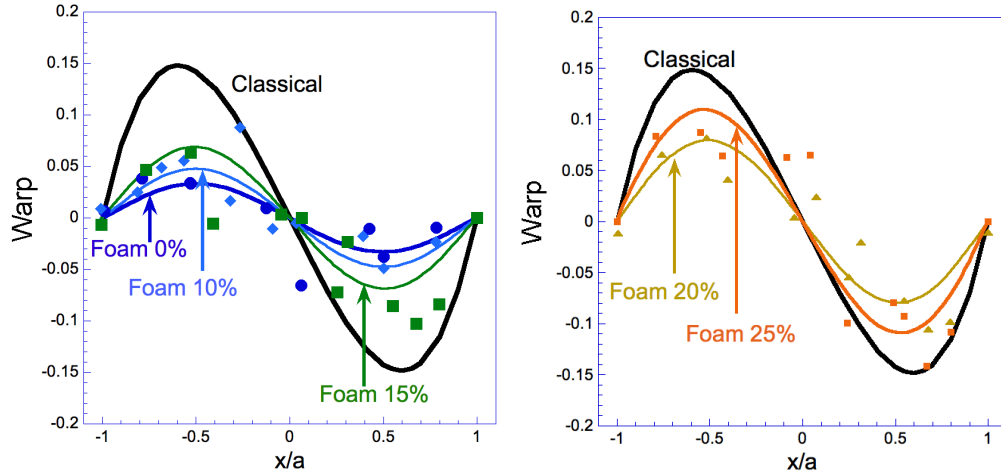
3   Results

Figure 3: Normalized warp $\frac{u_z(x,y)}{\theta a^2}$ in torsion of a square cross section bar for different amounts of axial pre-compression. Left, pre-compression 0% (circles), 10% (diamonds) and 15% (squares) vs. position. Points are experimental. Right, pre-compression 20% (triangles) and 25% (squares) vs. position. Curves are fits based on Cosserat elasticity with various characteristic lengths ℓ_t. The classical warp curve is shown for comparison

The energy stored by pre-compression is predicted to give rise to softening (reduction) of elastic constants. The degree of reduction, and whether negative values occur, is not known in advance.

Results of warp in torsion for 0%, 10% and 15% pre-compression strain are shown in Figure 3. Scatter of experimental points is due to non-affine deformation which is known to occur in foams such as this low density open cell foam. The density was 0.025 g/cm^3. Warp in all cases is considerably less than the classical prediction and is consistent with Cosserat elasticity. The inferred normalized characteristic lengths were $\bar{\ell}_t = \ell_t/a = 0.78$ with goodness of fit $R = 0.74$ and error 0.16 for the foam with no pre-compression. This $\bar{\ell}_t$ corresponds, with $a = 25$ mm, to $\ell_t = 20$ mm. This is about 3.3 times the cell size. For similar foams with smaller cells [24] studied via size effects, ℓ_t was about four times the cell size.

For 10% pre-compression strain $\bar{\ell}_t = 0.60$ with goodness of fit $R = 0.83$ and error 0.087; for 15% pre-compression strain, $\bar{\ell}_t = 0.43$ with $R = 0.80$ and error 0.084. Pre-compression in this range has the effect of increasing the warp as seen in the plot on the right in Figure 3 and of reducing the characteristic length.

For 20% pre-compression strain, $\bar{\ell}_t = 0.37$, with $R = 0.88$ and error 0.065. For 25% pre-compression strain, $\bar{\ell}_t = 0.23$, $R = 0.91$ and error 0.064. So this further axial pre-compression results in an additional increase in the warp as shown in shown in Figure 3 and reduces the characteristic length by more than a factor of three compared with the value $\bar{\ell}_t = 0.78$ for no pre-compression.

Further pre-compression to 27% led to more buckling and to chaotic warp deformation as shown in Figure 4. The points could not be well fitted by any theoretical warp curve, even by allowing Cosserat elastic constants in the unstable regime. Buckling from pre-compression is distinct from warp deformation because the initial value of position prior to the torsion experiment was taken after pre-compression and prior to torsion.
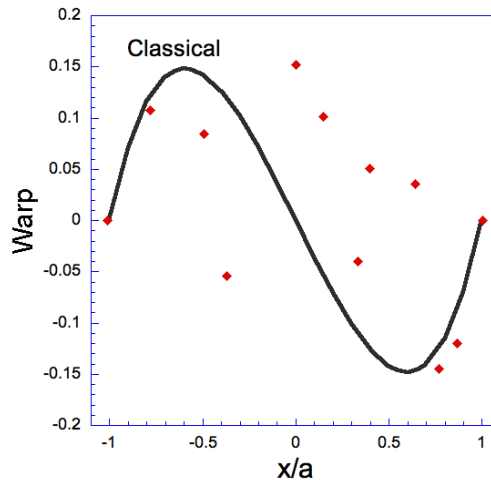

Figure 4: Normalized warp $\frac{u_z(x,y)}{\theta a^2}$ in torsion of a square cross section bar for axial pre-compression 27% vs. position. Points are experimental. The classical warp curve is shown for comparison.

4   Discussion

In addition to reducing stress concentrations [14] around holes, Cosserat elasticity increases the critical stress intensity factor as a measure of toughness [32]. Cosserat elasticity reduces the warp in the torsion of square cross section bars [30]; the concentration of strain is reduced as well.

Nonclassical warp observed in the torsion of foams implies a nonzero strain at the corners of the cross section, hence nonzero shear stress. The only way the shear stress can be nonzero at the corners is for it to be asymmetric. Asymmetry of the stress is permitted in Cosserat elasticity but excludes some other generalized continuum models. For example, the relaxed micromorphic model [33] has fewer elastic constants than the full micromorphic theory [18] [19] which has 18 isotropic elastic constants, but it assumes a symmetric stress. Nonclassical warp and observed phenomena at the corner of cross sections imply the stress must be asymmetric in these foams which can therefore be Cosserat elastic but not relaxed micromorphic.

As for stability of Cosserat solids, such generalized continua were compared with corresponding

analyses of lattice structures. It was suggested [34] that stability conditions weaker than those obtained from positive definite strain energy be used because they should be applied to volume elements substantially larger than the structural length scale of the material. Indeed, the variables used in positive definiteness analysis are coupled for objects of finite nonzero size, so stability conditions for Cosserat solids may not be so stringent as had been thought [15].

Recall that $\ell_t = \sqrt{\frac{\beta+\gamma}{2G}}$ so negative ℓ_t^2 implies negative $\beta + \gamma$. That is forbidden via the usual energy arguments but may be possible in an object of finite dimensions. The present experiments show, as anticipated, a reduction in ℓ_t with pre-compression hence a negative contribution to the initial value of $\beta + \gamma$ but they do not show any negative values of ℓ_t^2. So, the overall condition of positive definiteness is not violated in the inferred Cosserat moduli.

Instability can give rise to negative effective properties provided appropriate conditions are met. Also, a solid, if $N =1$, in the vicinity of the ellipticity criterion for stability can exhibit folding and faulting phenomena [35, 36, 37]. In the classical response of foams, buckling of ribs causes the curve of stress vs. strain to exhibit a small slope (the plateau region) compared with the linear elastic region. Individual cells exhibit a negative stiffness during compression [10] but the ensemble of cells comprising a sample of foam violates the condition of strong ellipticity. The foam exhibits bands of heterogeneous deformation; the foam stiffness is positive as rib buckling occurs. Hydrostatic compression, by contrast, allows one to observe a negative incremental bulk modulus [38] provided one controls the increment of volume rather than the pressure. It is not yet known what conditions are required to induce negative Cosserat parameters. Warp measurement provides a tool to explore such effects.

5   Conclusion

Warp of the cross sections of square bars of open cell foam is substantially reduced compared with classical predictions. The reduction of warp is consistent with Cosserat elasticity. Recovery of this warp and softening of the torsional Cosserat characteristic length in the foam material under compressive strain is observed.

6   Acknowledgements

References

[1] Bazant, Z., and Cedolin, L., Stability of Structures (Oxford University Press) 1991.

[2] Gibson, L. J. and Ashby, M. F., *Cellular Solids*, Pergamon, Oxford, 1988; 2nd Ed., Cambridge, 1997.

[3] I. S. Sokolnikoff, *Theory of Elasticity*, Krieger; Malabar, FL, (1983).

[4] L. D. Landau, in *Collected papers of L. D. Landau*, ed. D. Ter Taar, Gordon and Breach / Pergamon, New York, London (1965).

[5] R. S. Lakes, Extreme damping in compliant composites with a negative stiffness phase, Philosophical Magazine Letters, 81, 95-100 (2001).

[6] L. Dong and R. S. Lakes, Advanced damper with high stiffness and high hysteresis damping based on negative structural stiffness, Int. J. Solids Struct., 50, 2413-2423 (2013).

[7] R. S. Lakes, Extreme damping in composite materials with a negative stiffness phase, Physical Review Letters, 86, 2897-2900, (2001).

[8] R. S. Lakes, Lee, T., Bersie, A., and Wang, Y. C., Extreme damping in composite materials with negative stiffness inclusions, Nature, 410, 565-567, (2001).

[9] T. Jaglinski, Stone, D. S., Kochmann, D, and Lakes, R. S., Materials with viscoelastic stiffness greater than diamond, Science, 315, 620-622, (2007).

[10] Rosakis, P., Ruina, A., and Lakes, R. S., Microbuckling instability in elastomeric cellular solids, J. Materials Science, 28, 4667-4672 (1993).

[11] E. Cosserat and Cosserat, F., *Theorie des Corps Deformables*, Hermann et Fils, Paris (1909).

[12] R. D. Mindlin, Stress functions for a Cosserat continuum, Int. J. Solids Structures, 1, 265-271 (1965).

[13] A. C. Eringen, Theory of micropolar elasticity. In *Fracture*,1, 621-729 (edited by H. Liebowitz), Academic Press, NY, 1968.

[14] Mindlin, R. D., Effect of couple stresses on stress concentrations, Experimental Mechanics, **3**, 1-7, (1963).

[15] Lakes, R. S., Stability of Cosserat solids: size effects, ellipticity and waves, Journal of mechanics of materials and structures (JoMMS), 13 (1) 83-91 (2018).

[16] McKnight, R. E., Moxon, A. T., Buckley, A., Taylor, P. A., Darling, T. W. and Carpenter, M. A., Grain size dependence of elastic anomalies accompanying the alpha-beta phase transition in polycrystalline quartz, J. Phys. Cond. Mat. 20, 075229 (2008).

[17] Foamex Industries 1500 East 2nd Street, Eddystone, PA 19022, absorbed by FXI, 5 Radnor Corporate Center, 100 Matsonford Road, Radnor, PA 19087 `https://www.fxi.com/`

[18] Mindlin, R. D., Micro-structure in linear elasticity. Arch. Ration. Mech. Anal. 16, 51-78 (1964).

[19] Eringen, A.C., Suhubi, E.S., Nonlinear theory of simple micro-elastic solids - I. Int. J. Eng. Sci. 2(2), 189?203 (1964).

[20] J Jeong and P Neff, Existence, Uniqueness and Stability in Linear Cosserat Elasticity for Weakest Curvature Conditions, Mathematics and Mechanics of Solids, 15: 78-95, 2010.

[21] R. D. Gauthier and W. E. Jahsman, A quest for micropolar elastic constants. J. Applied Mechanics, 42, 369-374 (1975).

[22] D. Bigoni and W. J. Drugan, Analytical derivation of Cosserat moduli via homogenization of heterogeneous elastic materials, J. Appl. Mech., **74**, 741-753 (2007).

[23] Rueger, Z. and Lakes, R. S., Experimental study of elastic constants of a dense foam with weak Cosserat coupling, Journal of Elasticity 137(1), 101-115, (2019).

[24] Rueger, Z. and R. S. Lakes, Experimental Cosserat elasticity in open cell polymer foam, Philosophical Magazine, **96**, 93-111 (2016).

[25] Mora, R. and Waas, A. M., Measurement of the Cosserat constant of circular cell polycarbonate honeycomb, Philosophical Magazine A, **80**, 1699-1713 (2000).

[26] A. Spadoni and M. Ruzzene, Elasto-static micropolar behavior of a chiral auxetic lattice, J. Mechanics and Physics of Solids, **60**, 156-171 (2012).

[27] A.J. Beveridge, M.A. Wheel, D.H. Nash, The micropolar elastic behaviour of model macro-scopically heterogeneous materials, International Journal of Solids and Structures 50 246-255 (2013).

[28] A. Merkel and V. Tournat, Experimental Evidence of Rotational Elastic Waves in Granular Phononic Crystals, Phys. Rev. Lett., **107**(22), 225502 (2011).

[29] Rueger, Z. and Lakes, R. S., Strong Cosserat elasticity in a transversely isotropic polymer lattice, Physical Review Letters, 120, 065501 (2018).

[30] Drugan, W. J. and Lakes, R. S., Torsion of a Cosserat Elastic Bar with Square Cross-Section: Theory and Experiment, Zeitschrift fur angewandte Mathematik und Physik (ZAMP),69(2), 24 pages (2018).

[31] Lakes, R. S., Reduced warp in torsion of reticulated foam due to Cosserat elasticity: experiment, Zeitschrift fuer Angewandte Mathematik und Physik (ZAMP), 67(3), 1-6 (2016).

[32] Radi, E. On the effects of characteristic lengths in bending and torsion on Mode III crack in couple stress elasticity, International Journal of Solids and Structures **45**, 3033-3058, (2008).

[33] P. Neff, I. D. Ghiba. A. Madeo, L. Placidi, G. Rosi. A unifying perspective: the relaxed linear micromorphic continuum, Continuum Mech. Thermodyn. 26: 639-681 (2014).

[34] O. Brulin and Hjalmars, S., Stability conditions in continuum models of discrete systems, in Continuum Models of Discrete Systems 4, eds. O. Brulin and R. K. T. Hsieh, p. 209-212, North Holland Publishing, Amsterdam, 1981.

[35] P. A. Gourgiotis and Bigoni, D. (2016). Stress channelling in extreme couple-stress materials Part I: Strong ellipticity, wave propagation, ellipticity, and discontinuity relations. Journal of the Mechanics and Physics of Solids 88: 150-168.

[36] P. A. Gourgiotis, and Bigoni, D. (2016). Stress channelling in extreme couple-stress materials Part II: Localized folding vs faulting of a continuum in single and cross geometries. Journal of the Mechanics and Physics of Solids 88: 169-185.

[37] Gourgiotis, P. A., Bigoni, D., The dynamics of folding instability in a constrained Cosserat medium. Philosophical Transactions of the Royal Society A, A 375: 20160159 (2017).

[38] B. Moore, Jaglinski, T., Stone, D. S., and Lakes, R. S., Negative incremental bulk modulus in foams, Philosophical Magazine Letters, 86, 651-659, (2006).